

# Al-Doped Octahedral Cu<sub>2</sub>O Nanocrystal for electrocatalytic CO<sub>2</sub> Reduction to produce Ethylene

Sanxiu Li<sup>1,†</sup>, Xuelan Sha<sup>1,†</sup>, Xiafei Gao, Juan Peng<sup>1,\*</sup>

*1 State Key Laboratory of High-Efficiency Utilization of Coal and Green Chemical Engineering, College of Chemistry and Chemical Engineering, Ningxia University, Yinchuan 750021, China*

Correspondence: pengjuan@nxu.edu.cn

<sup>†</sup>The authors contribute equally to this work

## Chemicals and Reagents

The following chemicals were purchased and used without further purification: Copper chloride dihydrate (purity  $\geq 99.9\%$ , CuCl<sub>2</sub>·2H<sub>2</sub>O) powder was purchased from the Aladdin reagent network in China. Aluminum nitrate nine-hydrate (purity  $\geq 99.9\%$ , Al(NO<sub>3</sub>)<sub>3</sub>·9H<sub>2</sub>O), sodium hydroxide (purity  $\geq 99.9\%$ , C<sub>6</sub>H<sub>12</sub>O<sub>6</sub>), glucose (purity  $\geq 99.9\%$ , NaOH), potassium bicarbonate (purity  $\geq 99.5\%$ , KHCO<sub>3</sub>) was purchased from Sinopharm Chemical Reagent Co., Ltd in China. Nafion solution (5.0 wt%) was obtained from Tianjin Incole Union Technology Co., Ltd in China. Self-produced Deionized water. (18.24 MΩ cm<sup>-1</sup>) was used in the entire experiment.

## Characterization and measurement

Powder X-ray diffraction (XRD) measurements were conducted by a Smart Target X-ray diffractometer (Smart Lab, Japan). To observe the surface morphology of each electrocatalyst, we used an F-SEM cold field emission scanning electron microscope (F-SEM, Zeiss Sigma 300, Germany). High-resolution transmission electron microscope (HRTEM) and a high angle annular dark-field scanning transmission electron microscope (HAADFSTEM) was also used to obtain high-resolution images (FEI Talos F200x, America). Elemental content was analyzed by X-ray photoelectron spectroscopy (XPS, Thermo Scientific K-alpha, America),

using a monochromatic Al-K $\alpha$  radiation source (Mono Al-K $\alpha$ ) with 1486.6 eV of energy. Chemical states and surface material composition an X-ray photoelectron spectrometer was used for charge neutralization in the range of 75-150W with a low energy electron gun using a single cathode light source in a super-vacuum state. For the samples before electrocatalytic reaction, we directly characterize the freshly prepared electrodes. For the sample after electrocatalytic reaction, we washed the sample with deionized water, removed the surface electrolyte, and carried out characterization after drying.

## Density Functional Theory Simulation

We carried out all the DFT calculations in the Vienna *ab initio* simulation (VASP5.4.4) code[1]. The exchange-correlation is simulated with PBE functional and the ion-electron interactions were described by the PAW method[2, 3]. The vdWs interaction was included by using empirical DFT-D3 method[4]. The Cu<sub>2</sub>O (001) was heterocontacted with Cu (001) surface to simulate the catalysis of the reduction of CO<sub>2</sub> to CH<sub>2</sub>CH<sub>2</sub>. Atoms in the all the Cu (001) surface and upper two layers of the Cu<sub>2</sub>O (001) surface are allowed to move freely while the bottom two layers of Cu<sub>2</sub>O (001) surface are fixed to simulate the surface of structure. The Monkhorst-Pack-grid-mesh-based Brillouin zone k-points are set as 2 $\times$ 2 $\times$ 1 for all periodic structure with the cutoff energy of 400 eV. The convergence criteria are set as 0.01 eV A<sup>-1</sup> and 10<sup>-5</sup> eV in force and energy, respectively.

The free energy calculation of species adsorption ( $\Delta G$ ) is based on following model.

$$\Delta G = \Delta E + \Delta E_{ZPE} + \Delta H_{0 \rightarrow T} - T\Delta S \quad (1)$$

Herein  $\Delta E$ ,  $\Delta E_{ZPE}$ , and  $\Delta S$  respectively represent the changes of electronic energy, zero-point energy, and entropy that caused by adsorption of intermediate. The  $\Delta H_{0 \rightarrow T}$  refers to the change in enthalpy when heating from 0K to T K.

Table S1-1 Preparation conditions of catalyst

Catalyst	The concentration of Al <sup>3+</sup> (M)	The concentration of NaOH (M)	Time (min)	Remark
Cu <sub>2</sub> O	0	0.6	4	Optimum performance
Al-Cu <sub>2</sub> O	0.02	0.6	4	
Al-Cu <sub>2</sub> O-2	0.03	0.6	4	
Al-Cu <sub>2</sub> O-3	0.02	0.6	2	
Al-Cu <sub>2</sub> O-4	0.02	0.6	6	
Al-Cu <sub>2</sub> O-5	0.02	0.5	4	
Al-Cu <sub>2</sub> O-6	0.02	0.7	4	

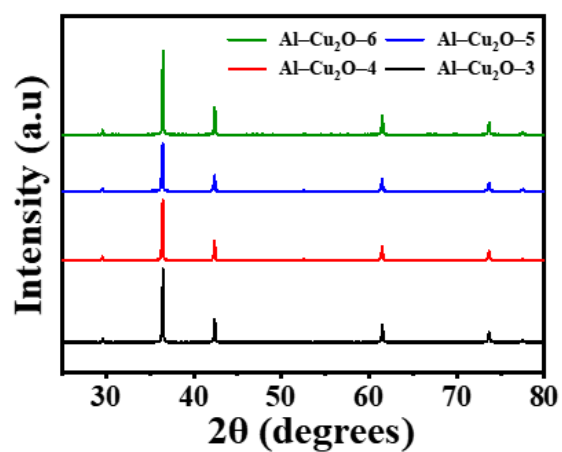


Figure. S1 XRD patterns of Al-Cu<sub>2</sub>O-X (X=3、4、5、6).

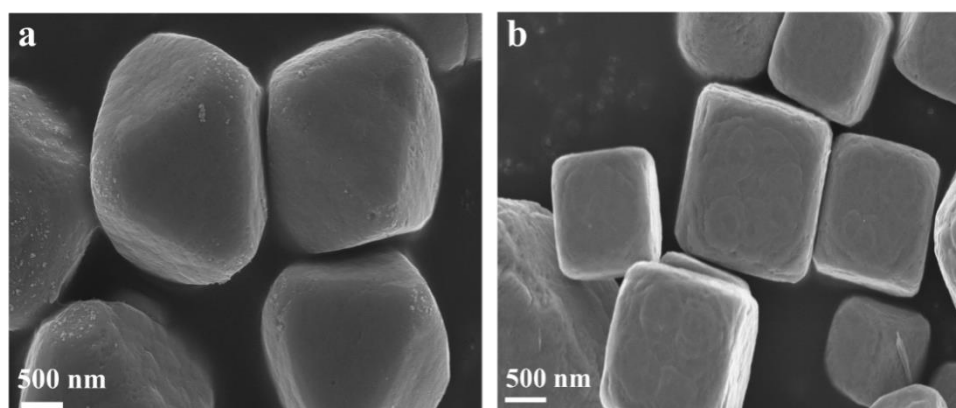


Figure. S2 SEM images of (a) Cu<sub>2</sub>O and (b) Al-Cu<sub>2</sub>O-2.

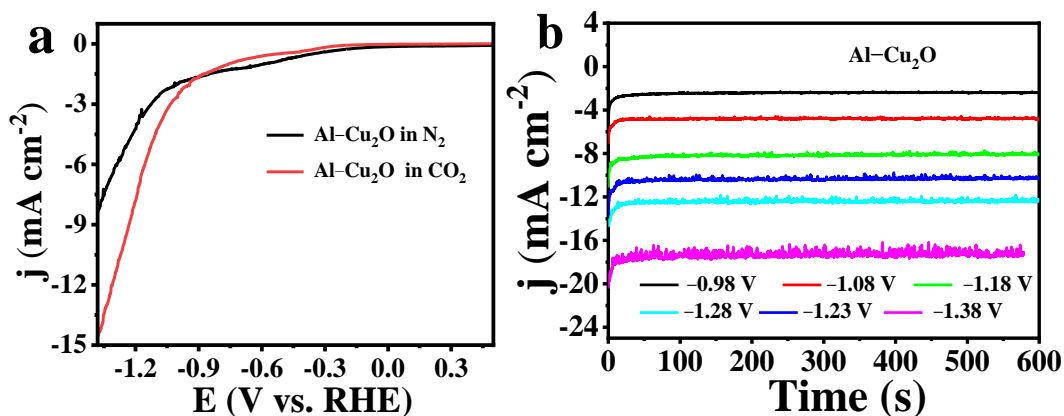


Figure. S3 (a) The polarization curves of Al–Cu<sub>2</sub>O catalyst in 0.1 M KHCO<sub>3</sub> aqueous solutions with saturated gases N<sub>2</sub> or CO<sub>2</sub> and (b) current response of Al–Cu<sub>2</sub>O in 0.1 M KHCO<sub>3</sub> saturated with CO<sub>2</sub>, sweeping speed of 5 mV s.

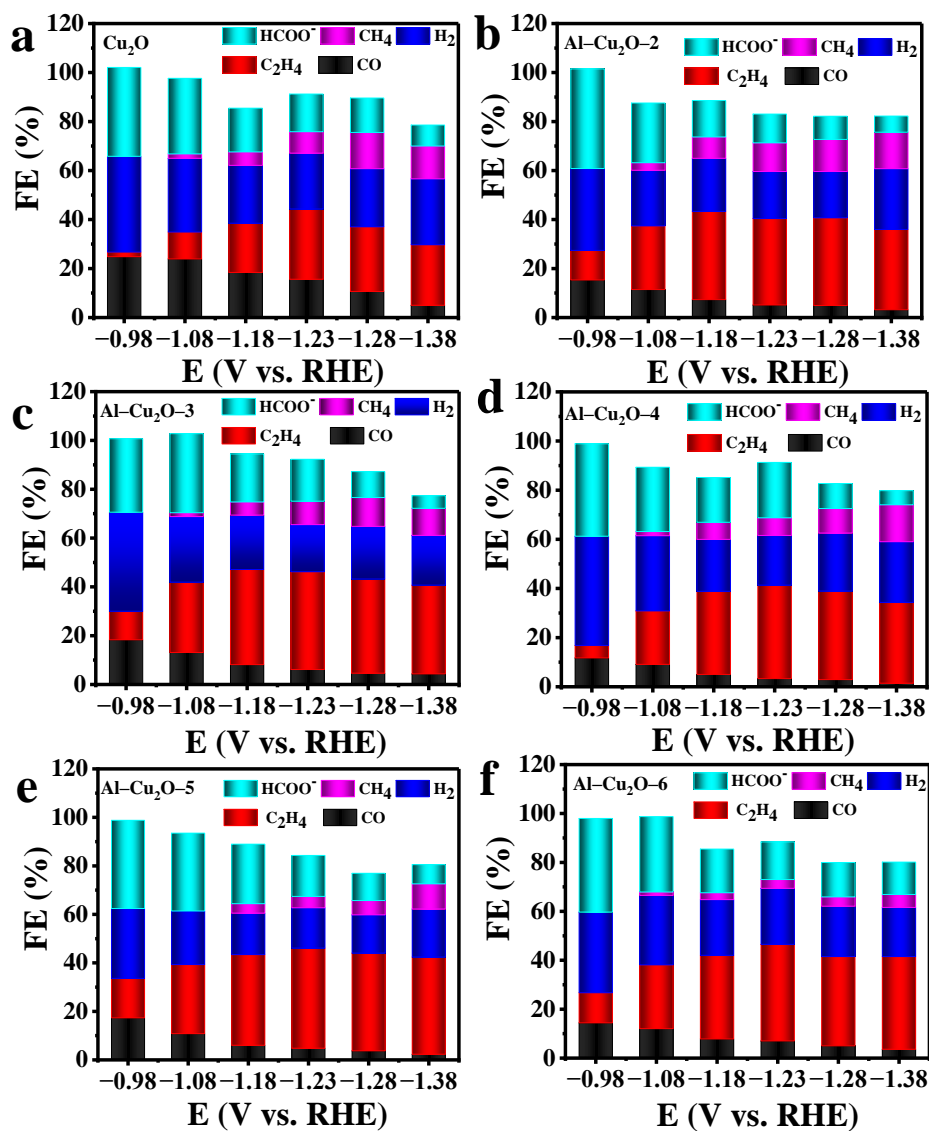


Figure. S4 (a-f) FE values of  $\text{Cu}_2\text{O}$  and  $\text{Al-Cu}_2\text{O-X}$  ( $X=2, 3, 4, 5, 6$ ) catalysts in 0.1 M  $\text{KHCO}_3$  aqueous solutions with saturated gas  $\text{CO}_2$ .

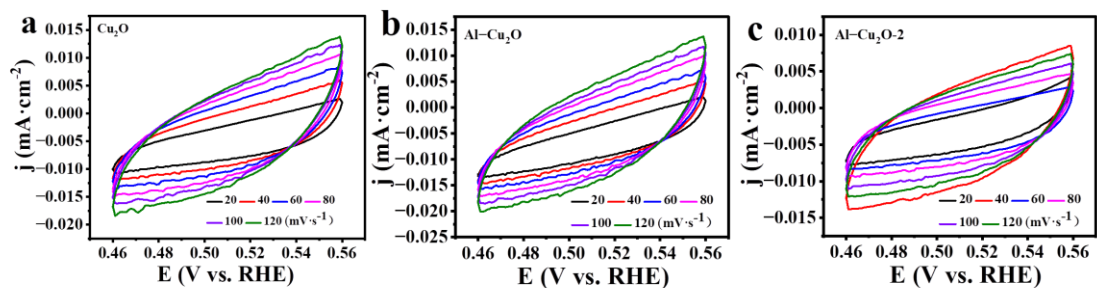


Figure. S5 The catalyst of (a)  $\text{Cu}_2\text{O}$ , (b)  $\text{Al-Cu}_2\text{O}$ , and (c)  $\text{Al-Cu}_2\text{O-2}$  volt-ampere curve in 0.1 M  $\text{KHCO}_3$  aqueous solutions with saturated gas  $\text{CO}_2$ ;

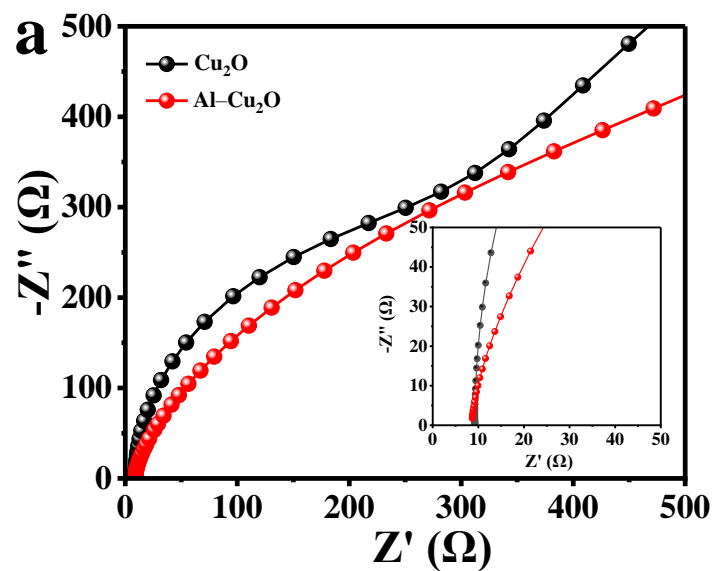


Figure. S6 (a) The EIS of  $\text{Cu}_2\text{O}$  and  $\text{Al-Cu}_2\text{O}$  catalysts.

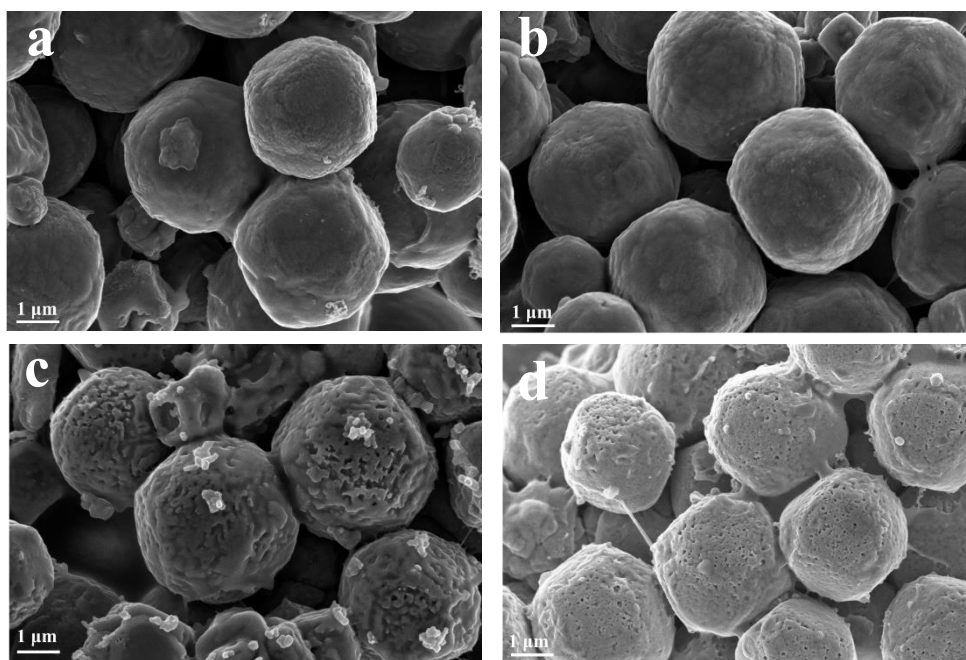


Figure. S7 Al-Cu<sub>2</sub>O catalyst in 0.1 M KHCO<sub>3</sub> electrolyte of Al-Cu<sub>2</sub>O catalyst in 0.1 M KHCO<sub>3</sub> electrolyte of SEM image (a) 0 min, (b) 20 min, (c) 0 min and (d) 7 h.

## References

1. Kresse, G.; Furthmüller, J. J. Efficient iterative schemes for ab initio total-energy calculations using a plane-wave basis set. *Phys. Rev. B*. **1996**, *54*, (16), 11169.
2. Perdew, J. P.; Burke, K.; Ernzerhof, M. J. Generalized gradient approximation made simple. *Phys. Rev. Lett.* **1996**, *77*, (18), 3865..
3. Hammer, B.; Hansen, L. B.; Nørskov, J. K. Improved adsorption energetics within density-functional theory using revised Perdew-Burke-Ernzerhof functionals. *Phys. Rev. B* **1999**, *59*, (11), 7413.
4. Grimme, S. J. Semiempirical GGA - type density functional constructed with a long - range dispersion correction. *J. Comput. Chem.* **2006**, *27*, (15), 1787-1799.